Influence of Surface Roughness on Wear Behaviour of Ceramic Nanocomposites

Nidhi Sharma*, Syed Nasimul Alam

Metallurgical and Materials Engineering Department, National Institute of Technology Rourkela, Rourkela, Orissa, Pin-769008, India

Abstract

The present work describes the influence of the surface roughness on the wear behaviour of Al_2O_3 and SiO_2 based nanocomposites, prepared with the reinforcement of exfoliated graphite nanoplatelets (xGnP) and multiwalled carbon nanotubes (MWCNT). The surface roughness for the pure sintered samples along with the various composites, reinforced with the different loading levels of xGnP and MWCNTs is determined by the scratch resistance test, using the stylus probe method. The average surface roughness (R_a) was determined by the scratch profiling technique using a stylus profilometer, having a diamond tip indenter. A detailed morphological investigation of the polished surface of the composites was carried out using an optical microscope and SEM. A clear transition in the roughness average (R_a) was observed for the composites, when the applied load was varied in the range of 1 to 3 mgf. Al_2O_3-xGnP and Al_2O_3-MWCNT nanocomposites having 0.2, 0.5, 0.8, 3 and 5 vol. % of the nanofillers and SiO_2-xGnP and SiO_2-MWCNT having 0.5, 1, 3 and 5 vol. % of the nanofillers were fabricated through the powder metallurgy route. SiO_2 based composites were sintered at 1350^{o}C for 4 h and for Al_2O_3 based composites, sintering was done at 1650^{o}C for 3 h. The effect of surface roughness on the wear behaviour of the nanocomposites was determined on the basis of the worn surface topography and wear debris analysis.

Keywords: Surface Roughness; Wear; Ceramic Nanocomposites; Graphite Nanoplatelets; Carbon Nanotubes

Introduction

Ceramics tend to be more rigid and brittle with potential hazard of excessive wear for most of the mechanical and electronic applications. On the other hand composite materials exhibit better mechanical properties and effective wear resistance with low abrasive nature. To understand the machinability of ceramic matrix composites (CMCs), the important factors to be considered include chip formation, machining forces, shear and friction angles and surface integrity. However, due to the complexity of the reinforcement mechanisms of the ceramic particles, a fair evaluation of the machinability of CMCs is still a difficult task. The dissemination of the nanostructured second phase particles, within the matrix or along the grain boundaries of the micron/submicron sized particles, leads to the prominent enhancement in the strength and fracture toughness. Improvement in the mechanical properties like hardness and better wear resistance of the ceramic nanocomposites could be achieved through the prolonged conventional sintering which makes them promising candidates, especially in the area of wear resistant applications [1]. Recent literature outlines the potential of CMCs in the tribological and machining applications. Si_3N_4/BN nanocomposites were found to possess higher fracture strength and better machinability, when compared with the similar microcomposites having a superior surface finish as exhibited by the machined components [2]. Nanocrystalline WC-Co composites were reported to have much higher wear resistance (~four times), and more than double the lifetime, in cutting applications when compared to the conventional coarse-grained composite materials [3]. This attributes to their exceptional mechanical properties like toughness and hardness. Substantial work has been accomplished to develop CMCs and a lot of reports are available in the literature on their potential properties and applications [4]. However, research reports to understand the tribological properties of the CMCs are rather confined. Recently, the tribological behaviour of Al_2O_3/SiC and Si_3N_4/SiC nanocomposites have been investigated in the literature. Davidge et al. analysed the erosive wear behaviour of Al_2O_3/SiC nanocomposites against Al_2O_3 ball [5] whereas, Dusza et al. [6] described the wear and friction behaviour of Si_3N_4/SiC ceramic nanocomposites against Si_3N_4 ball, using a pin-on-disc wear tester. The wear rate of polycrystalline Al_2O_3 was notably reduced by the dispersal of secondary SiC nanoparticles and various smooth transgranular fracture paths were observed in the worn composites. The sliding wear properties of Al_2O_3/SiC nanocomposites by varying the grain size of SiC were studied by Rodriguez et al [7]. Intergranular fracture followed by the grain pull-out were demonstrated as the ascendant wear mechanisms. The present study is carried out to investigate the influence of surface roughness on the wear behaviour of SiO_2- xGnP/MWCNT and Al_2O_3-xGnP/MWCNT nanocomposites.

2. Materials and Methods

2.1 Synthesis of Nanofillers

2.1.1 Exfoliated Graphite Nanoplatelets (xGnP)

Exfoliated graphite nanoplatelets (xGnP) were synthesized via. intercalation process, using sulfuric acid (H_2SO_4) between the layers of the natural flake graphite (NFG), along with hydrogen peroxide (H_2O_2). H_2SO_4 is a strong mineral acid with

dehydrating and oxidizing property while H_2O_2 is thermodynamically unstable and is a strong oxidizer. NFG having a mean size of 60 mesh and purity of 98% was procured from Loba Chemie, India. H_2O_2 and H_2SO_4 (98%) were contrived from Merck, India. All reagents used had the highest commercially available purity and were of analytical grade. 1.5 ml of H_2O_2 (30%) and 16 ml of concentrated H_2SO_4 (98%) were mixed with 6 gm of NFG to obtain a graphite intercalation compound (GIC), also known as the expanded graphite. The solution was magnetically stirred for 2 h. The black filtrate was then treated with distilled water for about 5 times to remove all the ionic and acidic impurities and a pH value in the range of 5-7 was attained. The GIC was then dried overnight in air and then further dried at 60^oC in a muffle furnace for 8 h to remove any remaining moisture to obtain a completely dry resultant powder. The residual powder was then followed up with a thermal shock at 1000^oC for 30 seconds in a muffle furnace, consequently forming the thermally exfoliated graphite. Later 1 gm of the thermally exfoliated graphite was mixed with 100 ml of acetone in a closed setup to prevent acetone evaporation and ultrasonicated for 20 h. After ultrasonication, the beaker containing the xGnPs was kept at room temperature in air, to evaporate all the remaining acetone and finally the resultant dry xGnP was collected.

2.1.2 Multi Walled Carbon Nanotubes (MWCNT)

The MWCNTs were grown using a LPCVD technique. For the synthesis of MWCNTs, Fe-thin film catalyst was encrusted on the Si substrate using RF sputtering (12'' MSPT) at Ar pressure of 10^{-3} Torr and power of 50 W. The thickness of the Fe catalyst film observed was ~15 nm. The sputtered film was cleaned ultrasonically in acetone and dried at room temperature before loading into a quartz tube and was heated to a high temperature under H_2 flow. A mixture of H_2:C_2H_2:NH_3 with flow rates of 20:50:20 sccm respectively, was introduced into the quartz tube. The reaction temperature was kept at 900^oC and the growth time was 20 min. A continuous Ar gas was fed at a controlled rate of 600 sccm during the entire heating up, growth and cooling down periods for preventing the oxidation and removal of gaseous by-products. Due to the Van der Waals forces and high aspect ratio, the MWCNTs tend to agglomerate. Acid functionalization of the MWCNTs has been done in order to avoid the agglomeration of the MWCNTs and enhance their dispersion in the matrix. The MWCNTs were stirred in an acidic solution containing H_2SO_4 and HNO_3 in 3:1 ratio with 50% acid concentration, using a magnetic stirrer for a period of 8 h. The MWCNTs were then filtered and repeatedly washed with distilled water to attain the pH value of 7. Further, MWCNTs were dried in a vacuum oven at 80^oC for a period of 5 h. The presence of hydroxyl (-OH) and carboxyl (-COOH) groups, introduced during functionalization prevented the Van der Waals forces between the MWCNTs to overcome the clustering and agglomeration.

2.2 Fabrication of Composites
2.2.1 Al_2O_3-Based Nanocomposites

Powder processing route was opted to develop the Al_2O_3-xGnP/MWCNT composites to achieve homogeneous dispersion of the nanofiller in the Al_2O_3 matrix. For the development of the composites, alumina (α-Al_2O_3) powder was procured from RFCL Limited, India. The Al_2O_3/xGnP and Al_2O_3/MWCNT were ultrasonicated in acetone for 2 h in the desired ratio to prepare individual slurry. The slurry was then ball milled at 150 rpm for 30 minutes in a Fritsch Pulverisette 5 planetary ball mill using zirconia (ZrO_2) milling media. Milling was done using ZrO_2 balls having a diameter of 20 mm with a ball to powder weight ratio of 10:1. Toluene was used as the wetting media during milling. Later the milled slurry was dried by heating at a temperature of 80^oC for 12 h. The dried mixture was ground by mortar and pestle to get a fine and evenly mixed Al_2O_3-xGnP and Al_2O_3-MWCNT powders, which were again subjected to heating at 80^oC in a vacuum oven for another 7 h , to get the completely dried powder mixtures. In order to find out the effect of the addition of xGnP and MWCNT on the various properties, pure Al_2O_3 sample was also fabricated via. same processing route for reference. Al_2O_3-xGnP and Al_2O_3-MWCNT composites were devolved from their respective blended powder mixtures. Pure Al_2O_3 and Al_2O_3-0.2, 0.5, 0.8, 3 and 5 vol.% xGnP and Al_2O_3-0.2, 0.5, 0.8, 3 and 5 vol.% MWCNT composites were developed by conventional sintering carried out at 1650^oC in inert Ar atmosphere for a holding time of 3h under the load of ~390 MPa.

2.2.2 SiO_2-Based Nanocomposites

Powder processing route was opted for the development of SiO_2-xGnP/MWCNT composites, so that uniform dispersion of the nanofillers in the SiO_2 matrix could be achieved. Silica (SiO_2) powder in 100-200 mesh size was procured from Thermo Fischer Scientific Pvt. Limited, India. The xGnP used was ultrasonicated for 20h before its introduction into SiO_2 matrix and MWCNTs were functionalised as described above. The SiO_2-xGnP and SiO_2-MWCNT powder mixtures were ultrasonicated in acetone for 3 h in the desired ratio to prepare the individual slurry. The slurry was then ball milled at 150 rpm for 30 minutes in a Fritsch Pulverisette 5 planetary ball mill using zirconia (ZrO_2) milling media. Milling was done using ZrO_2 balls having a diameter of 20 mm with a ball to powder weight ratio of 10:1. Toluene was used as the wetting media during milling. Later the milled slurry was dried by heating at a temperature of 100^oC for 5 h. The dried mixture was ground by mortar and pestle to get a fine and evenly mixed SiO_2-xGnP and SiO_2-MWCNT powders which were again subjected for heating at 100^oC in a vacuum oven for 5 h , to get a completely dried powder mixture.SiO_2-xGnP and SiO_2-MWCNT composites were devolved from the blended powder mixtures. Pure SiO_2 and SiO_2-0.5, 1, 3 and 5 vol.% xGnP and SiO_2-0.5, 1, 3 and 5 vol.% MWCNT composites were developed by conventional sintering carried out at 1350^oC in inert Ar atmosphere for holding time of 4h under a load of ~310 MPa.
The Archimedes' method was used to determine the bulk density of the various composites, and their theoretical density was calculated by the rule of mixture assuming the density of Al_2O_3 as 3.95 gm/cc, density of SiO_2 as 2.65 gm/cc, density of xGnP as 2.26 gm/cc and the density of MWCNT as 2.6 gm/cc respectively for the various nanocomposites. After consolidation, the upper

surface of various sintered Al_2O_3/SiO_2 based nanocomposites were polished using fine grain paper, followed by diamond cloth polishing. The polished and scratch free composite surfaces were observed under an optical microscope. The morphology and elemental composition of the various composites were analysed using a SEM equipped with EDX.

3. Experimental

In the present work, the effect of nano-reinforcement on the wear behaviour of CMCs is reported. Profilometry results and weight loss of the composites after wear test are analysed to co-relate their effect on the nanocomposites. Results suggest that the surface topography and the magnitude of normal applied force on the composites produce a significant change in average surface roughness (R_a) and thus vary the wear resistance of the composites. Therefore, this study is aimed to assess the effect of normal applied load and the surface roughness of the nanocomposites on the wear behaviour of the CMCs. The average surface roughness, R_a , is the amount of prominent elevations and depressions measured on the composite surface in a cross-section. It is arithmetic average of the divergence of absolute values of the profile height from the mean line , measured within the evaluated length [8].Surface roughness was measured through a scratch profiling technique using diamond tip indenter of stylus profilometer (Veeco Dektak 150). Scratched surfaces were viewed under Veeco Innova Scanning Probe Microscope, to analyse the tribological behaviour of the nanocomposites. Stylus tip having a diameter of 1.25 µm was used to give the normal load of 1, 2, 3 mg in three consecutive runs for each composite for a fixed length of 3000µm for observation time of 200 sec. The value of R_a was recorded in Å. Dry sliding wear test of the pure sintered Al_2O_3 and SiO_2 samples along with the various Al_2O_3-xGnP/MWCNT and SiO_2-xGnP/MWCNT composites was carried out to determine their wear performance. To investigate the wear mechanism, a ball-on-plate type tribometer (DUCOM TR208-M1) having a diamond indenter of 2 mm diameter, with a normal applied load of 1 Kgf for a sliding time of 10 minutes at a sliding speed of 20 rpm was used for each sintered sample. A wear track of 6 mm diameter was formed on the surface of the composites. The test was carried out at room temperature and the variation of wear depth and the wear rate with the sliding time was plotted for the various samples.

4. Results and Discussion

Strength, hardness and chemical stability of ceramic materials is determined by the strong ionic or covalent bonds between their atoms. On the other hand, composite materials exhibit better mechanical properties and effective wear resistance with low abrasive nature. In abrasive applications, where corrosion resistance, high strength, and refractoriness is needed, ceramics with enhanced tribological properties are preferred. Thus to improve the tribological properties and to amplify the different mechanical behaviours of monolithic ceramics , nanofillers like graphene (and its derivatives) and carbon nanotubes (CNT) are introduced to form CMCs. It has been reported that both graphene and CNT provide ideal lubrication and reduce wear. Exfoliated graphite nanoplatelets (xGnP) acts as the solid lubricant having a lamellar structure. This layered structure promotes the sliding movement of the parallel planes. Multi walled carbon nanotubes (MWCNTs) are carbon allotropes having a tubular and cylindrical structure. Graphene and carbon nanotubes (CNT) reinforced composites have been reported to have higher fracture toughness as compared to the monolithic ceramics [9].

To ascertain the features in nanometer domain, Conventional HRTEM images (operating at 300 kV) of as-prepared exfoliated graphite nanoplatelets (xGnPs) were analyzed. A low magnification HRTEM image of the bulk xGnP having multilayered graphene sheets have been shown in Fig.1 (a). In Fig.1 (b), giant overlapped graphite nanoplatelets can be seen overlapping each other. The graphite nanoplatelets are also found to be electron transparent. As the 2D membrane structure becomes thermodynamically stable by bending, corrugation and scrolling are part of the inherent nature of graphene nanosheets [10]. HRTEM was also used to analyze the structure of MWCNTs. The HRTEM images of the MWCNTs in Figs. 1(c, d) are found to have diameter of a few nanometers. Many black dots on the edges of CNTs are observed (Fig.1(c)), which are the agglomerated bundles of MWCNTs adhering to the sidewalls of long MWCNTs. The SAD pattern of the xGnP recorded along the [001] zone axis in Fig.1 (e), shows that the xGnP have a well crystallized graphite structure [11]. The crystalline nature of the xGnP could be confirmed by the spots observed in the diffraction pattern, fully indexed to the hexagonal graphite crystal structure. The SAD pattern in Fig.1 (f) confirms the crystallinity of the MWCNTs due to their hexagonal pattern which clearly indicates the six-fold symmetry of carbon atoms organised in the graphite lattice.

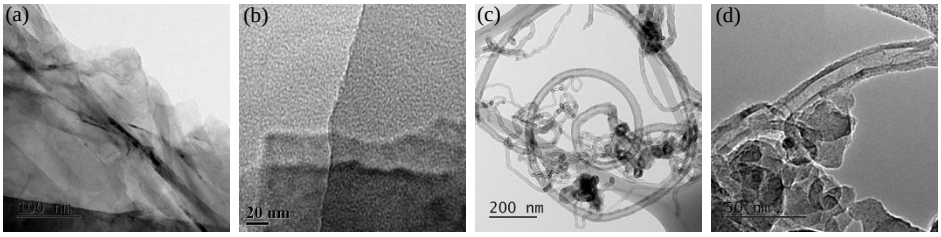

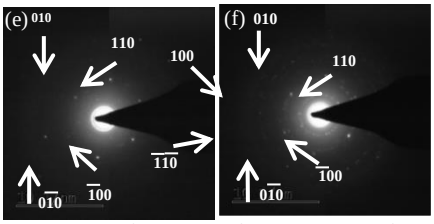

Fig.1. HRTEM images of (a, b) xGnP; (c, d) MWCNT; SAD pattern of (e) xGnP; (f) MWCNT used for the development of SiO_2/Al_2O_3 based nanocomposites

The extent of defects in carbonaceous materials can be determined by Raman spectroscopy analysis. Fig.2 shows the Raman spectra of xGnP and MWCNTs. The Raman spectrum of xGnP developed by 20 h ultrasonication of the thermally exfoliated graphite (xGnPs) is shown in Fig.2 (a). The two most intense peaks observed in the spectrum are the G band at ~1580 cm^{-1} and the 2D band at ~2700 cm^{-1}. The G peak emerges due to the bond stretching of all pairs of sp_2 atoms in both chains and the rings. The G and 2D Raman peaks change in shape, position and relative intensity with the number of graphene layers in the graphite platelets [12]. Peaks at 1350 cm^{-1} (D) and 1620 cm^{-1} (D') reveal defects in the xGnP sample. The Raman spectra of the MWCNTs is presented in Fig.2 (b), where two peaks appear at ~1330 cm^{-1} (D-band) and ~1580 cm^{-1} (G-band). The D-band represents the disordered or sp_3 hybridized carbons in the MWCNT walls and the G-band corresponds to vibrations of sp_2 bonded carbon atoms present in the MWCNTs [13]. The intensity ratio of the D band to G band (ID/IG) can serve as an appropriate measurement to estimate the amount of defects in the graphitic lattice. The value of ID/IG ratio for the xGnP and MWCNT is 0.171 and 0.296 respectively. This ensures that the structural integrity of the nanofillers is maintained with negligible defects in them.

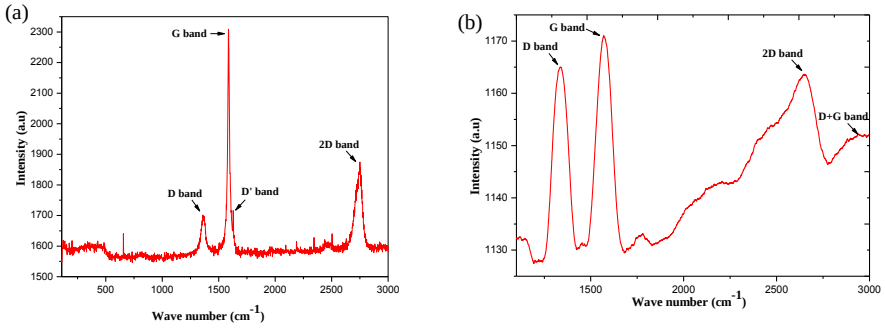

Fig.2. Raman spectra of (a) xGnP; (b) MWCNT

Fig.3 shows the HRTEM images of SiO_2-xGnP/MWCNT and Al_2O_3-xGnP/MWCNT milled powder mixtures having 3 vol. % loading level of the nanofiller. The Al_2O_3 and SiO_2 powders were blended with nanofillers by ball milling for a short period of time. There was no evident structural and morphological damage to the MWCNTs after wet milling of the powder mixture. MWCNTs were mainly found to be located at the grain boundaries of the ceramic particles, well adhered with the matrix. Multi-layered stacks of xGnP and agglomerates of CNTs could be visualised from the HRTEM images. Fine silica and alumina particles having nanometric dimension are clearly evident in the HRTEM images. The SAD pattern in Figs.3 (e-h), indicate the six-fold symmetry of the xGnP and the MWCNTs. The concentric rings in the SAD pattern are due to the silica or alumina particles which could be broken down to nanometric level during milling [14].

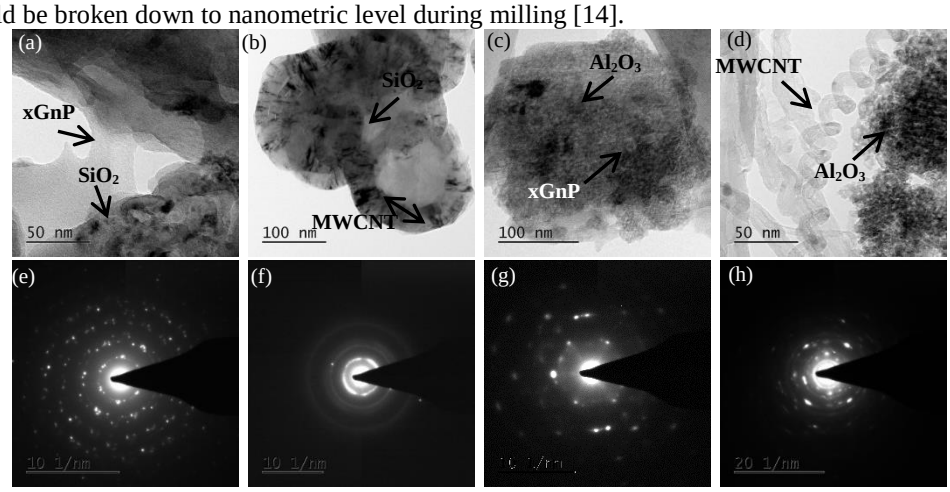

Fig.3. HRTEM images of (a) SiO_2-3vol.% xGnP; (b) SiO_2-3vol.% MWCNT; (c) Al_2O_3-3vol.% xGnP; (d) Al_2O_3-3vol.% MWCNT and SAD patterns of (e) SiO_2-3vol.% xGnP; (f) SiO_2-3vol.% MWCNT; (g) Al_2O_3-3vol.% xGnP; (h) Al_2O_3-3vol.% MWCNT powder mixtures

The microstructure of various SiO_2-xGnP/MWCNT nanocomposites sintered for 4 h and Al_2O_3-xGnP/MWCNT nanocomposites sintered for 3 h are shown in Fig.4. The silica-xGnP/MWCNT grain size ranges between 900 nm-1.3 µm whereas the grain size of alumina in the Al_2O_3-xGnP/MWCNT composites is ~1.5µm. The SEM images in Figs.4 (b, c) and Figs.4 (g, h) show well distributed xGnP in the SiO_2/Al_2O_3 matrix after prolonged sintering. Prominent shape change and varied grain growth can be

seen for SiO_2/Al_2O_3 matrix particles. The grain growth behaviour of CMCs are intensely affected by the nanofillers and crucially dependent on sintering duration. Addition of nanofiller restricts the grain growth of both the SiO_2/Al_2O_3 based composites by grain pinning. MWCNTs were not evenly distributed over the surface of the Al_2O_3 matrix, suggesting that grain growth occurs at specific locations in the Al_2O_3 matrix. SEM images in Figs.4 (d, e) clearly show MWCNTs at the grain boundaries of the SiO_2 matrix. The bridge connecting two particles in Fig.4 (i) is composed of stacks of aligned CNTs, indicating that the CNTs originated from one of the Al_2O_3 grains and end on another grain [15]. Nanofillers when added at lower loading levels uniformly fill the pores in the composites without any agglomeration leading to homogenous grain growth and densification.

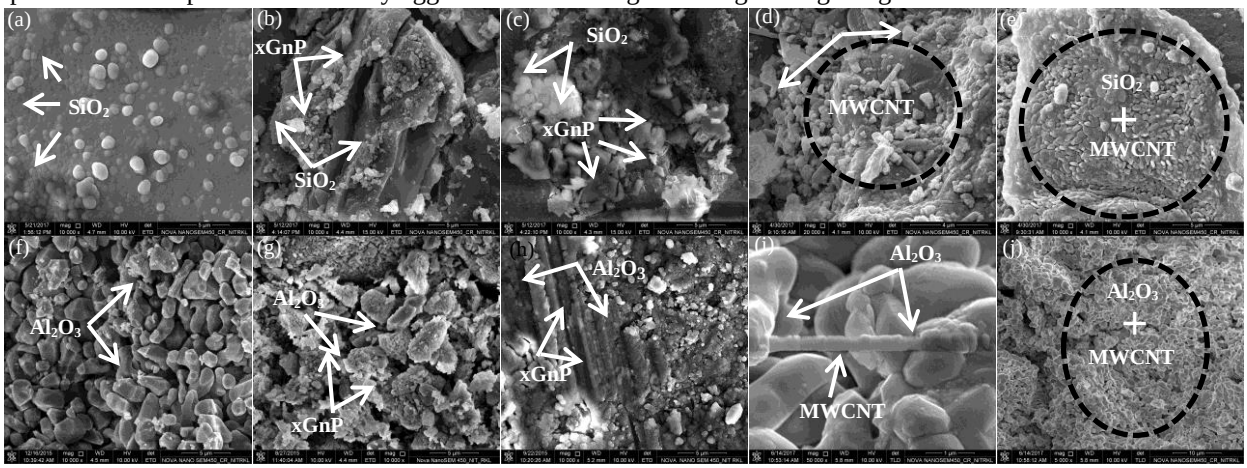

Fig.4. (a) Pure SiO_2; (b, c) SiO_2-3 vol.% xGnP; (d, e) SiO_2-3 vol.% MWCNT nanocomposite and (f) Pure Al_2O_3; (g, h) Al_2O_3-3vol.% xGnP; (i, j) Al_2O_3-3vol.% MWCNT nanocomposite

Both SiO_2-xGnP/MWCNT and Al_2O_3-xGnP/MWCNT composites with varied loading levels of nanofillers behave differently during the profilometry test depending on the applied normal load. In the case of SiO_2 based composites, it is evident from Fig.5 (a), that the R_a values of the composites do not change significantly when loading level of xGnP was increased to 0.5 vol.% in SiO_2 matrix for the applied load of 1, 2, 3 mgf. However, the R_a value continuously increases when xGnP is increased from 0.5 vol. % to 5 vol. %. The average roughness of SiO_2-xGnP composites is found to increase on increasing the applied load from 1 mgf to 3 mgf when xGnP content in the SiO_2 matrix is increased. Similar results are obtained for SiO_2-MWCNT composites in Fig.5 (b). However, in the case of SiO_2-xGnP composites a major effect of the normal load variation from 1 mgf to 3 mgf was observed when xGnP loading level was above 1 vol. % whereas in the case of SiO_2-MWCNT composites, this behaviour was observed when the MWCNT concentration was below 1 vol. %. The value of R_a was found to increase with the increase of the normal applied load for both SiO_2-xGnP/MWCNT composites. Both xGnP and MWCNT provide lubricity to the rough ceramic matrix when added at a lower loading level of upto 5 vol. % and consequently, result in lower abrasion and better wear resistance of the sintered composites. As the normal load increases, the scratch resistance of the xGnP and MWCNT reinforced composites decreases due to the presence of weakly bonded grain boundaries in the ceramic matrix, which enhances chipping of materials [16]. For both SiO_2-5 vol. % xGnP and SiO_2-5 vol. % MWCNT composites, R_a is maximum for 3 mgf and minimum for 1 mgf normally applied load whereas the minimum value of R_a was observed for SiO_2-0.5 vol. % xGnP and SiO_2-0.5 vol. % MWCNT composite on application of 1 mgf normal load.

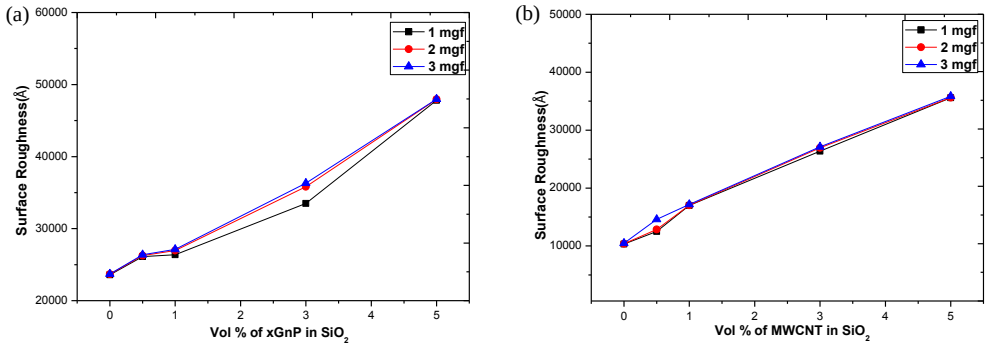

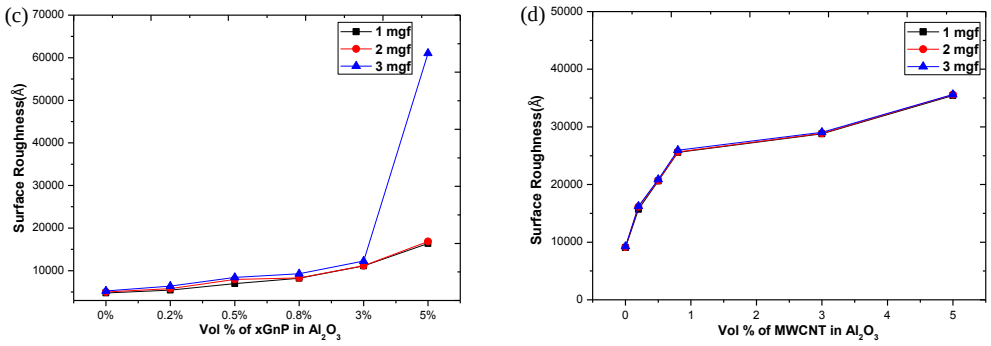

Fig.5. R_a profile for (a) SiO_2-xGnP composites; (b) SiO_2-MWCNT composites sintered at 1350°C for 4 h and (c) Al_2O_3-xGnP composites; (d) Al_2O_3-MWCNT composites sintered at 1650°C for 3 h, at the normal applied loads of 1, 2 and 3 mgf

In the case of Al_2O_3-xGnP/MWCNT composites, R_a value simultaneously increases with the increase in loading level of the nanofillers from 0.5 vol. % to 5 vol. % on varying the normally applied load from 1 mgf to 3 mgf. However, the pattern of increment in R_a value is different for Al_2O_3-xGnP and Al_2O_3-MWCNT composites. In Fig.5 (c), a drastic increase in R_a is observed when the applied load is increased from 1 mgf to 3 mgf for Al_2O_3-5 vol. % xGnP composite. The minimum value of R_a is observed for the normal applied load of 1 mgf for all the composites, irrespective of their composition. The increase in surface roughness of the Al_2O_3-xGnP composites at a higher loading level of xGnP in Al_2O_3 matrix could be attributed to the increased brittleness index of the composites. High loads during the scratch test, due to the presence of weakly bonded grains in CMCs, produce more extensive chipping as compared to monolithic ceramics. This suggest that low loading levels of xGnP upto 0.5 vol. % for SiO_2-xGnP composites and upto 0.2 vol.% for Al_2O_3-xGnP composites, are beneficial for improving the scratch resistance. In Fig. 5(d), a similar pattern in the increment of R_a was observed for all composition of Al_2O_3-MWCNT composites, suggesting a uniform effect of MWCNTs on the abrasive properties of the matrix, irrespective of the loading levels and extent of load application. This is in accord with SiO_2-MWCNT composites where a similar behaviour was observed (Fig. 5(b)). It implies that the effect of the normal applied load is not prominent for roughness measurement in MWCNT reinforced composites, whereas, it is remarkably significant in the case of xGnP reinforced composites, for both SiO_2 and Al_2O_3 systems. Overlapping of xGnPs and MWCNTs at the grain boundaries lead to the formation of weakly bonded grains. The nanofillers have a high aspect ratio and are bonded by weak Van der Waals forces [17].

Variation in the hardness of various SiO_2-xGnP/MWCNT and Al_2O_3-xGnP/MWCNT composites has been shown in Fig.6. It is evident from the plots in Fig.6, that among the two CMCs, SiO_2 based composites have a higher hardness when reinforced with either xGnP/MWCNT. The highest hardness value is obtained at the loading level of 3 vol. % for both the nanofillers, in the case of both SiO_2 and Al_2O_3 based composites. The deterioration in hardness when the loading level of the nanofiller is increased beyond 3 vol. %, is caused due to the clustering and agglomeration of the nanofiller in the ceramic matrix. For the SiO_2-3vol. % xGnP composite, the hardness was found to be ~7.51 GPa which is ~3.2 times higher than the hardness of the Al_2O_3-3vol. % xGnP composite (~2.34 GPa). It should be noted that the silica based composites show a finer grain size as compared to the alumina based nanocomposites which could result in the higher hardness of the silica based nanocomposites. Stronger grain-growth retardation was observed in the case of SiO_2 based composites. Similarly, for the SiO_2-3vol. % MWCNT composite, the hardness value was recorded ~7.45 GPa which is ~1.8 times higher than that observed in the case of Al_2O_3-3vol. % MWCNT composite (~4.1 GPa). Although, it should be noted, that there is almost negligible difference in the hardness value of SiO_2-3 vol. % xGnP and SiO_2-3vol. % MWCNT composites when both are developed under similar conditions. On the contrary, the hardness value of Al_2O_3-3 vol. % MWCNT composite is ~1.7 times higher than that observed in the case of Al_2O_3-3 vol. % xGnP composite. It is noteworthy, that both the xGnP and MWCNT contribute towards the hardness improvement of the monolithic SiO_2 and Al_2O_3 at the lower loading levels. Lower loading levels of the nanofillers lead to uniform dispersion of the nanofillers in the ceramic matrix resulting in the better hardness of the composites [18].

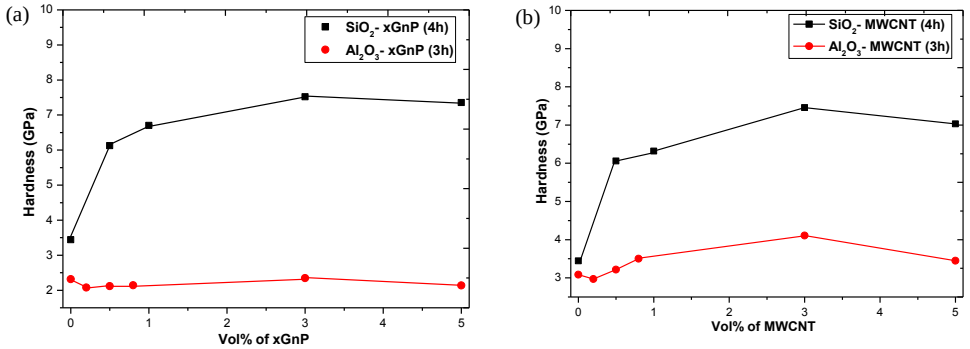

Fig.6. Variation in hardness for (a) SiO_2 /Al_2O_3- xGnP composites; (b) SiO_2 /Al_2O_3- MWCNT nanocomposites

Signs of composite wear include abrasion, micro-cracks and damages due to residual stresses, increased surface roughness, microscopic changes of surface morphology and fatigue. Composite wear is affected by factors such as structure of the material like geometrical properties, size, volume of filler etc., interaction conditions including force, stress, time, and surface texture which include chemical surface topography, temperature etc. [19]. As evident from Fig.7, CMCs having MWCNT as nanofiller are more prone to wear than xGnP reinforced composites. In Fig.7 (a), the lowest wear rate for SiO_2-xGnP composites was observed for sample having 3 vol.% loading level of xGnP whereas for Al_2O_3-xGnP system, Al_2O_3-0.8 vol. % xGnP composite was found to have the highest wear resistance. However, on further increment in the xGnP loading level beyond 3 vol. %, wear rate remarkably increases due to the agglomeration of the nanofiller in the ceramic matrix. On the other hand, wear behaviour of the SiO_2-MWCNT composites was found to be rather different. SiO_2-MWCNT composites show better wear resistance when the loading level of MWCNT was maintained in between 1 vol. % to 3 vol. % which further decreases when MWCNT content is increased upto 5 vol. %. The maximum wear rate observed for SiO_2-5 vol. % MWCNT composite is ~2.86 x 10^{-4} g/Nm which is ~57% higher than that observed for SiO_2-5 vol. % xGnP composite (~1.82 x 10^{-4} g/Nm). The minimum wear rate of SiO_2-3 vol. % xGnP composite was recorded as ~1.3 x 10^{-4} g/Nm which is ~28.5% higher than the wear rate observed in the case of SiO_2-3 vol. % MWCNT composite (~1.82 x 10^{-4} g/Nm). On introduction of xGnP/MWCNT into the Al_2O_3 matrix, wear rate continuously improves giving the maximum wear resistance in case of Al_2O_3-0.8 vol. % xGnP and Al_2O_3-0.8 vol. % MWCNT composites as ~1.08 x 10^{-4} g/Nm and ~1.06 x 10^{-4} g/Nm respectively. It is noticeable that introduction of nanofillers like xGnP/MWCNT, provide better wear resistance than the monolithic ceramic samples upto the loading level of 5 vol. %. Furthermore, it should be noted that SiO_2-xGnP/MWCNT composites provide better wear resistance than Al_2O_3-xGnP/MWCNT composites when developed under similar conditions. Figs.7 (c, d) show the variation in wear depth for various SiO_2-xGnP/MWCNT and Al_2O_3- xGnP/MWCNT composites. In Fig.7 (c), Al_2O_3-xGnP composites show a rather irregular and fluctuating wear depth as compared to SiO_2-xGnP composites. For SiO_2-xGnP composites, wear depth was lesser as compared to monolithic SiO_2 whereas for Al_2O_3-0.2 vol. % xGnP and Al_2O_3-3 vol. % xGnP composites, the wear depth was higher as compared to the pure sintered Al_2O_3 sample. However, MWCNT reinforced CMCs do not exhibit this behaviour. Better wear resistance was observed for both SiO_2- MWCNT and Al_2O_3- MWCNT composites when compared to pure SiO_2 and Al_2O_3 samples.

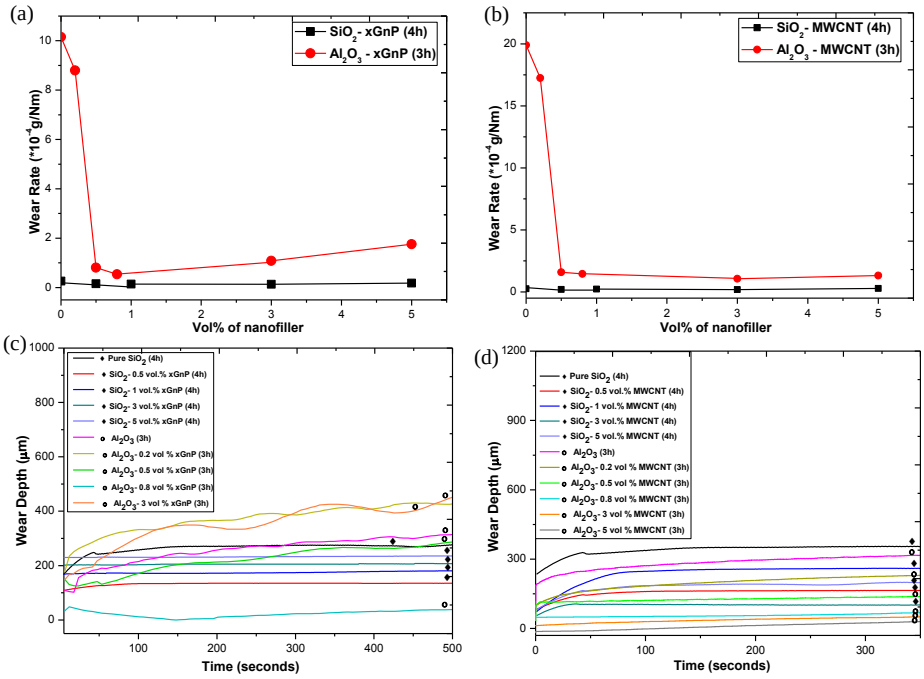

Fig.7. Variation in wear rate of (a) SiO_2/Al_2O_3- xGnP; (b) SiO_2/ Al_2O_3-MWCNT nanocomposites and wear depth of (c) SiO_2/ Al_2O_3- xGnP; (d) SiO_2/ Al_2O_3-MWCNT nanocomposites

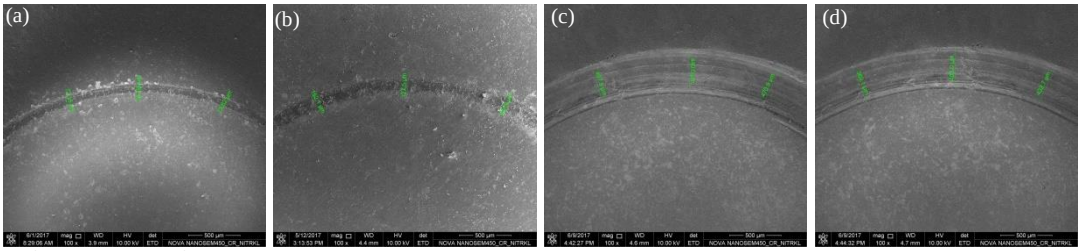

Fig.8. SEM images of the wear track of (a) SiO_2-3vol.% xGnP; (b) SiO_2-3vol.% MWCNT; (c) Al_2O_3-3vol.% xGnP; (d) Al_2O_3-3vol.% MWCNT nanocomposites

It is evident that MWCNT reinforced composites show more homogeneous wear depth as compared to the composites having xGnP as nanofiller. Also SiO_2 matrix serves as a better host for xGnP/MWCNT to improve the wear resistance. Similar results are observed from the wear tracks shown in Fig.8. Average diameter of the wear track for SiO_2-xGnP/MWCNT composites is much less than that for Al_2O_3- xGnP/MWCNT composites.

5. Conclusion

Wear resistance is a major concern for mechanical behaviour of the composites. Depending upon the extent of wear, restoration of the composites to its previous mechanical condition may not be possible due to the variation in surface roughness. The results of the present study show:

1. Increase in the normal applied load increases the weight loss and result in the significant wear. The friction between the composite surface and the stylus tip is effective on the wear behaviour. Greater forces result in higher friction coefficient and thereby increase the wear. Also, during the contact between the indenter and material surface, some filler particles are rubbed off while some others are pressed into the surface and as a result, wear and particle aggregation occur at the same time.
2. The wear is affected by geometric parameters such as the texture of the abrasive surface and contact area. Under higher loads, the bond between the composite filler and matrix becomes more sensitive to degradation. Particle pull-out facilitates chip breaking and affects the R_a value.
3. Regardless of the material type, a change in the value of R_a could be observed even when the applied load is as significantly less as 1 mgf. As polished surface is smoother, it has lower surface roughness and the friction between the composite and stylus tip reduces. Analysis of the data showed that weight loss for 3 mgf loaded samples was significantly more than that of 1 mgf.
4. Matrix type, shape, size, volume and distribution of nanofillers, filler hardness are the factors that affect the wear behaviour of the nanocomposite. Nanofillers like xGnP and MWCNTs are found to be very effective in improving the wear resistance of the composites when added at a lower loading level of upto 3 vol. %.
5. SiO_2-xGnP/MWCNT composites were found to have a better wear resistance as compared to Al_2O_3-xGnP/MWCNT composites when developed under the similar conditions.

Acknowledgements

We cordially acknowledge the support provided by the FESEM Laboratory of the Ceramic Engineering Department, HRTEM Laboratory of the Chemical Engineering Department of NIT Rourkela for their sincere support. We also thank the Physics Department and the Central Research Facility, IIT Kharagpur for their sincere support.

References

[1] P. Palmero, F. Kern, F. Sommer, M. Lombardi, R. Gadow, L. Montanaro, J. Appl. Biomater. Funct. Mater. 12(3) (2014) 113–128.
[2] T. Kusunose, T. Sekino, Y.H. Choa, K. Niihara, J. Am. Ceram. Soc. 85(11) (2002) 2689–95.
[3] C. Suryanarayana, Int. Mater. Rev. 40(2) (1995) 41–64.
[4] S. Komarneni, J. Mater. Chem. 2 (1992) 1219–30.
[5] R.W. Davidge, P.C. Twigg, F.L. Riley, J. Eur. Ceram. Soc. 16 (1996) 700–802.
[6] M. Kagiarova, E. Rudnayova , J. Dusza, M. Hnatko, P. Sajgalık, A. Merstallinger, L. Kuzsella, J. Eur. Ceram. Soc. 24 (2004) 3431–5.
[7] J. Rodriguez, A. Martin, J. Y. Pastro, J. L. Lorce, J. F. Bartlome, J. S. Moya, J. Am. Ceram. Soc. 82(8) (1999) 1252–4.
[8] W. M. Huitt, Bioprocessing Piping and Equipment Design: A Companion Guide for the ASME BPE Standard, John Wiley & Sons, 2016, pp. 59.
[9] B. Yazdani, F. Xu, I. Ahmad, X. Hou, Y. Xia, Y. Zhu, Sci. Rep. 5 (2015) 11579.
[10] Y. Chen, Z. Hu, Y. Chang, H. Wang, Z. Zhang, Y. Yang, H. Wu, J. Phys. Chem. C. 115 (2011) 2563–2571.
[11] P.M. Ajayan, S. Iijima, Nature 358 (1992) 23.
[12] A.C. Ferrari, J.C. Meyer, V. Scardaci, C. Casiraghi, M. Lazzeri, F. Mauri, S. Piscanec, D. Jiang, K.S. Novoselov, S. Roth, A.K. Geim, Phys. Rev. Lett. 97 (2006) 187401.
[13] M.S. Dresselhaus, A. Jorio, A.G. Souza, R. Saito, Phil. Trans. R. Soc. A. 368 (2010) 5355-5377.
[14] E.I. Suvorova, F. Christensson, H.E.L. Madsen, A.A. Chernov, J. Cryst. Growth.186 (1998) 262-274.
[15] K.R. Al-Rawi, H. Adawiya, O.A. Mahmood, Int. J. App. Inn. Eng. Mng. 3(8) (2014) 132-137.
[16] EA. Tsitrou, S.E. Northeast, R.V. Noort, J. Dent. 35 (2007) 897-902.
[17] H. Porwal, M. Kasiarova, P. Tatarko, S. Grasso, J. Dusza, M.J. Reece, Adv. Appl. Ceram., 114(1) (2015) 34-41.
[18] H. Conrad, J. Narayan, Scripta. Mater. 42 (11) (2000) 1025–30.
[19] C.P. Turssi, B.M. de Purquerio, M.C. Serra, J. Biomed. Mater. Res. B. Appl. Biomater. 65(2) (2003). 280–5.